



Published in final edited form as:

*Nat Neurosci.* ; 15(1): 113–122. doi:10.1038/nn.2993.

## Coactivation of Thalamic and Cortical Pathways Induces Input Timing-Dependent Plasticity in Amygdala

Jun-Hyeong Cho<sup>1</sup>, Ildar T Bayazitov<sup>2</sup>, Edward G Meloni<sup>1</sup>, Karyn M Myers<sup>1</sup>, William A Carlezon Jr.<sup>1</sup>, Stanislav S Zakharenko<sup>2</sup>, and Vadim Y Bolshakov<sup>1</sup>

<sup>1</sup>Department of Psychiatry, McLean Hospital, Harvard Medical School Belmont, Massachusetts 02478

<sup>2</sup>Department of Developmental Neurobiology St. Jude Children's Research Hospital Memphis, Tennessee 38017

### Abstract

Long-term synaptic enhancements in cortical and thalamic auditory inputs to the lateral nucleus of the amygdala (LAN) mediate encoding of conditioned fear memory. It remained unknown, however, whether the convergent auditory conditioned stimulus (CSa) pathways may interact with each other producing changes in their synaptic function. Here we show that continuous paired stimulation of thalamic and cortical auditory inputs to the LAN with the interstimulus delay approximately mimicking a temporal pattern of their activation in behaving animals during auditory fear conditioning results in persistent potentiation of synaptic transmission in cortico-amygdala pathway in rat brain slices. This novel form of input timing-dependent plasticity (ITDP) in cortical input depends on InsP<sub>3</sub>-sensitive Ca<sup>2+</sup> release from the internal stores and postsynaptic Ca<sup>2+</sup> influx through calcium-permeable kainate receptors during its induction. ITDP in the auditory projections to the LAN, determined by characteristics of presynaptic activity patterns, may contribute to the encoding of the complex CSa.

### INTRODUCTION

The lateral nucleus of the amygdala is a brain structure integrating conditioned and unconditioned (UCS) stimuli during fear conditioning<sup>1,2</sup>. Both cortical and thalamic inputs, arising from the auditory cortex and the auditory thalamus, respectively, deliver the CSa information to the LAN and support fear learning<sup>3</sup>. It has been suggested, however, that these two routes of the CSa delivery could differ in their contributions to the acquisition of fear memory in the intact brain<sup>4</sup>. Thus, the cortical areas contribute more significantly to the processing of complex CSa<sup>5</sup>. Signals transmitted by direct projections from the auditory

Users may view, print, copy, download and text and data- mine the content in such documents, for the purposes of academic research, subject always to the full Conditions of use: [http://www.nature.com/authors/editorial\\_policies/license.html#terms](http://www.nature.com/authors/editorial_policies/license.html#terms)

\*Correspondence should be addressed to V.Y.B. (vadimb@mclean.harvard.edu).

Note: Supplementary Information is available on the Nature Neuroscience website.

#### AUTHOR CONTRIBUTIONS

J.H.C., I.T.B., E.G.M., K.M.M., W.A.C., S.S.Z. performed the experiments and analyzed the results. V.Y.B. and J.H.C. designed the experiments, interpreted the results and wrote the paper.

thalamic areas reach the LAN earlier than those arriving from the auditory cortex<sup>6-9</sup>. Consistent with the role of behaviorally-induced plasticity in the direct thalamo-amygdala pathway in fear learning, fear conditioning was found to be associated with significant enhancements of the short-latency auditory responses, reflecting inputs from the auditory thalamus, in LAN neurons in freely moving rats<sup>8</sup>. Subsequent experiments provided extensive evidence that the mechanisms of long-term potentiation (LTP) in both cortico- and thalamo-amygdala pathways could mediate memory of the CSa-UCS association during fear conditioning<sup>10-14</sup>.

The ability of synapses in both thalamic and cortical inputs to undergo LTP independently<sup>15</sup> is likely to reflect the sufficiency of either projection for fear learning<sup>3</sup>. Nevertheless, based on results of the experiments in freely moving rats, it has been suggested that associative interactions between two auditory inputs to the LAN could lead to the mutual synaptic strengthening in the CSa pathways<sup>16</sup>. However, synaptic mechanisms of such potential interactions between convergent thalamic and cortical inputs to the LAN have not been previously explored. We started addressing these questions by studying the functional consequences of the paired stimulation of cortical and thalamic projections in brain slices with the protocol resembling a temporal pattern of their activation *in vivo*. We found that the time-locked sequential activation of convergent auditory projections to the LAN induces input timing-dependent plasticity (ITDP; ref. 17) at the cortico-amygdala synapses.

## RESULTS

### Priming thalamic afferents induces ITDP in cortical input

We activated thalamic or cortical inputs to principal neurons in the LAN in brain slices, placing stimulation electrodes onto the internal capsule or the external capsule, respectively<sup>12, 15,18-23</sup> (Supplementary Fig. 1a,b and Fig. 1a, see Online Methods). Excitatory postsynaptic currents (EPSCs) were recorded under whole-cell voltage-clamp conditions at a holding potential of  $-70$  mV in the presence of the  $\gamma$ -aminobutyric acid receptor A (GABA<sub>A</sub>R) antagonist picrotoxin (50  $\mu$ M). With our stimulation techniques, thalamic and cortical projections to the LAN were activated independently, as the arithmetic sum of the amplitudes of the EPSCs evoked by stimulation of either cortical or thalamic inputs separately was nearly identical to the EPSC amplitude when both inputs were stimulated simultaneously<sup>15</sup> (Supplementary Fig. 1c,d). Moreover, we did not observe cross-facilitation between the inputs, as stimulation of the cortical input with a single stimulus had no effect on the amplitude of the EPSC in the thalamic input evoked with a 50-ms delay, and vice versa (Supplementary Fig. 1e,f).

Previous *in vivo* recordings indicate that the signal from the auditory thalamus arrives to the LAN  $\sim 15$ – $20$  ms earlier than that from the auditory cortex<sup>9,24,25</sup>. This is because the auditory information eventually entering the LAN from the cortex is transmitted to the thalamus first, is next conveyed to the TE3 area of the auditory cortex, and only then is relayed to the LAN<sup>21,25</sup>. To investigate whether these two CSa pathways interact to affect synaptic responses in LAN principal neurons, we designed a stimulation protocol approximately mimicking the temporal relation of their activation in animals. It implicated continuous paired stimulation of the thalamic and cortical afferents with single presynaptic stimuli (TSt

and CSt, respectively), delivered in such a manner that thalamic input was activated 15 ms prior to the stimulation of cortical input (TSt-CSt pairing protocol;  $t = -15$  ms; Fig. 1b).

Paired stimulation of the thalamic and cortical inputs for 90 s at a 1 Hz frequency, while the recorded postsynaptic neuron was voltage-clamped at a holding potential of  $-70$  mV, resulted in significant potentiation of the EPSC amplitude in the cortico-amygdala pathway (Fig. 1c,e). The amplitude of the EPSCs evoked by stimulation of the thalamic input, however, remained unaltered (Fig. 1d,f). The induction of potentiation in cortical input required priming stimulation of thalamic fibers, because stimulation of the cortical input alone at either 1-Hz (for 90 s) or 2-Hz (for 45 s) frequencies had no effect on the amplitude of cortico-LAN EPSCs (Fig. 1g,h and Supplementary Fig. 2, respectively). Under current-clamp recording conditions, when the postsynaptic membrane was allowed to depolarize during the induction, the TSt-CSt pairing protocol also induced potentiation of the excitatory postsynaptic potentials (EPSPs) in the cortical input to the LAN (Supplementary Fig. 3a,b). Temporal summation of the thalamic and cortical EPSPs, observed during the pairing of thalamic and cortical stimuli with a short interstimulus interval (15 ms), resulted in the averaged peak somatic depolarization of  $10.1 \pm 1.3$  mV ( $n = 6$ ), which did not lead to the spike firing in a recorded postsynaptic neuron (Supplementary Fig. 3a). Together, these findings indicate that the delivery of the TSt-CSt pairing protocol induces input timing-dependent potentiation (ITDP)<sup>17</sup> in the cortico-amygdala pathway.

Neurons in the LAN receive massive inhibitory inputs from the local circuit GABA-releasing interneurons<sup>26–28</sup>, controlling the susceptibility of synapses to LTP<sup>22,29–31</sup>. We found, however, that the magnitude of ITDP in cortical input, induced in the absence of the GABA<sub>A</sub>R receptor antagonist picrotoxin in the external medium (Supplementary Fig. 3c,d), was not different from that observed when inhibition was blocked (as shown in Fig. 1e;  $t$  test,  $P = 0.11$ ). These results demonstrate that GABA<sub>A</sub>R-mediated inhibition does not have a significant impact on ITDP induction.

### Time interval between TSt and CSt controls ITDP magnitude

We next examined whether the inducibility of ITDP depends on the time interval between activation of thalamic and cortical inputs during paired stimulation. When the time interval between TSt and CSt was increased to 30 ms or 60 ms ( $t = -30$  ms or  $t = -60$  ms, respectively), the TSt-CSt pairing did not result in ITDP in cortical input (Fig. 2a,d,e). On the other hand, paired stimulation of thalamic and cortical inputs with  $t = -8$  ms resulted in potentiation of the cortico-amygdala EPSC (Fig. 2a and Supplementary Fig. 4a). The magnitude of potentiation under these conditions was not significantly different from ITDP induced with  $t = -15$  ms ( $t$  test,  $P = 0.84$ ). The TSt-CSt stimulation with  $t = -8$  ms also led to potentiation in the “priming” pathway (thalamic input) (Fig. 2b and Supplementary Fig. 4a), whereas the induction protocol with  $t = -15$  ms resulted in ITDP in cortico-amygdala input only (Fig. 2c). Simultaneous activation of thalamic and cortical inputs ( $t = 0$  ms) resulted in potentiation of both the cortico-amygdala and thalamo-amygdala EPSCs (Fig. 2a,b and Supplementary Fig. 4b). Thus, although ITDP in projections to the LAN could be induced at the inter-input stimulation intervals shorter than 15 ms, the pathway specificity of ITDP is only maintained at the 15-ms delay between activation of thalamic and cortical

fibers. These findings indicate that the inducibility and pathway-specificity of ITDP in the LAN is determined by the temporal delay between thalamic and cortical signals.

Reversing the temporal order of paired stimulation of cortical and thalamic pathways (the CSt-TSt protocol) was associated with potentiation of the thalamo-amygdala EPSCs ( $t = +15$  ms; Fig. 2b,f), whereas EPSCs in cortical projections did not exhibit significant enhancements. Following the delivery of the CSt-TSt stimulation with  $t = +8$  ms, potentiation was observed in both thalamic and cortical inputs (Fig. 2a,b; Supplementary Fig. 4c). The CSt-TSt pairing with a longer interval ( $t = +30$  ms) did not induce an increase of the EPSC amplitude either in thalamic or cortical inputs (Fig. 2b,g). These results show that both cortical and thalamic projections to the LAN possess the ability to undergo ITDP. However, ITDP in cortical input, induced by the TSt-CSt pairing, is likely to be more functionally relevant, as it may reflect the temporal order in which thalamic and cortical afferents are activated *in vivo*.

### Glutamate uptake maintains pathway specificity of ITDP

Active glutamate uptake maintains input specificity of the conventional pairing-induced LTP in auditory inputs to the LAN, preventing heterosynaptic plasticity<sup>15</sup>. We explored the role of glutamate uptake in the induction of ITDP in the LAN, delivering the TSt-CSt pairing stimulation protocol ( $t = -15$  ms) at room temperature (22°C–25°C). Glutamate transporters are highly temperature-sensitive and their functional efficiency is significantly diminished under such conditions<sup>32</sup>. In these experiments, the magnitude of ITDP was not different from the ITDP magnitude induced at more physiological temperatures (Supplementary Fig. 5a,e; *t* test,  $P = 0.58$ ).

This potentiation, however, was no longer pathway specific, as the EPSC in thalamic input was also potentiated (Supplementary Fig. 5b,e). Moreover, following blockade of glutamate transporters with a specific inhibitor DL-TBOA (10  $\mu$ M) at physiological temperatures, the delivery of the TSt-CSt stimulation resulted in similar potentiation of the EPSC amplitude in cortical input (Supplementary Fig. 5c,e) and “priming” thalamic pathway (Supplementary Fig. 5d,e;  $P = 0.62$  for potentiation at cortical input versus potentiation at thalamic input; *t* test). Therefore, an efficient removal of released glutamate by glutamate transporters is required for maintaining pathway specificity of ITDP in the LAN.

### Requirements for the induction of ITDP in the LAN

In the presence of the high affinity  $\text{Ca}^{2+}$  chelator BAPTA (10 mM) in the recording pipette solution, the TSt-CSt pairing protocol (with a 15-ms interval) did not lead to the induction of ITDP at the cortico-amygdala synapses (Fig. 3a,b), indicating that the rise in postsynaptic  $\text{Ca}^{2+}$  concentration is required for the induction process. Both N-methyl-D-aspartate receptors (NMDAR) and L-type voltage-gated  $\text{Ca}^{2+}$  channel were previously identified as the sources of postsynaptic  $\text{Ca}^{2+}$  increases, triggering different forms of LTP in the LAN<sup>12,15,22,33,34</sup>. Surprisingly, the induction of ITDP in the LAN did not depend on NMDAR activation, as it was not suppressed by the NMDAR antagonist D-2-amino-5-phosphonopentanoic acid (D-AP5, 50  $\mu$ M; not significantly different from control ITDP,  $P = 0.64$ ; Fig. 3c,i), while NMDAR EPSCs were completely blocked by the antagonist at this

concentration (Supplementary Fig. 6a,b). The L-type  $\text{Ca}^{2+}$  blocker nitrendipine (20  $\mu\text{M}$ ) also had no effect on ITDP when applied alone (Fig. 3d,i) or jointly with D-AP5 (Supplementary Fig. 7a–c,g). We also re-tested the effects of D-AP5 on ITDP in the LAn recoding synaptic responses in a current-clamp mode, thus allowing depolarization of the postsynaptic neuron during the TSt-CSt pairing. ITDP of the EPSPs in cortical input to the LAn was still not blocked in the presence of D-AP5 (Supplementary Fig. 6c,d; not significantly different from ITDP induced in the absence of D-AP5, as shown in Supplementary Fig. 3a,b;  $P = 0.49$ ). These findings show that the postsynaptic  $\text{Ca}^{2+}$  influx, required for the induction of ITDP in the LAn, is not mediated by activation of NMDARs or L-type  $\text{Ca}^{2+}$  channels.

What are the cellular mechanisms implicated in the induction of ITDP in the LAn? Kainate glutamate receptors (KARs), specifically the GluR5 (GluK1) subunit-containing receptor complexes, are highly expressed in the amygdala<sup>35</sup>. KARs were shown previously to mediate the induction of a form of LTP in the basolateral amygdala<sup>35</sup>, as well as LTP at the mossy fiber synapses in the hippocampus<sup>36</sup>. In our experiments, ITDP in cortical input was completely blocked in the presence of either UBP 296 (5  $\mu\text{M}$ ) or ACET (10  $\mu\text{M}$ ), the specific antagonists of GluR5 KARs (Fig. 3e,i; Supplementary Fig. 7d,g), indicating the role for these receptors in the induction process. GluR5 subunit-containing KARs were implicated in the induction of heterosynaptic potentiation in thalamic input in the presence of DL-TBOA (10  $\mu\text{M}$ ) at physiological temperatures as well since this potentiation was blocked by UBP 302 (Supplementary Fig. 5f).

Similar to hippocampal ITDP<sup>17</sup>, ITDP in cortical input to the LAn was suppressed in the presence of the group I mGluR antagonists CPCCOEt (40  $\mu\text{M}$ ) and MPEP (20 $\mu\text{M}$ ) (Fig. 3f,i) (blocking mGluR1 and mGluR5 receptors, respectively) or LY 367385 (100  $\mu\text{M}$ ) and SIB 1757 (30  $\mu\text{M}$ ) (Supplementary Fig. 7e,g). The induction of ITDP was unaffected, however, by the antagonist of muscarinic acetylcholine receptors atropine (1 $\mu\text{M}$ ; Supplementary Fig. 7f,g). Release of  $\text{Ca}^{2+}$  from the internal stores is implicated, under certain conditions, in the induction of LTP<sup>37,38</sup>, and, specifically, ITDP<sup>17</sup> at central synapses. Consistent with the role of  $\text{Ca}^{2+}$  release from the internal stores in ITDP induction, we found that ITDP in the amygdala was blocked when Xestospongine-C (10  $\mu\text{M}$ ), which inhibits  $\text{InsP}_3$ -sensitive  $\text{Ca}^{2+}$  stores, was included in pipette solution (Fig. 3g,i). However, ITDP was not affected by ryanodine (100  $\mu\text{M}$ ), blocking ryanodine receptor-mediated  $\text{Ca}^{2+}$  release (Fig. 3h,i).

The addition of a specific agonist of GluR5-containing KARs (RS)-2-amino-3-(3-hydroxy-5-tert-butylisoxazol-4-yl)propanoic acid (ATPA, 1  $\mu\text{M}$ ) to the external solution did not result in potentiation of the cortico-amygdala EPSCs (Fig. 4a,d). The bath-applied agonist of group I mGluRs (S)-3,5-dihydroxyphenylglycine ((S)-DHPG, 10  $\mu\text{M}$ ) also had no effect on the EPSC in cortical input (Fig. 4b,d). However, when applied together, ATPA and (S)-DHPG produced synaptic potentiation (Fig. 4c,d), indicating the need for a joint activation of both GluR5 KARs and group I mGluRs. Consistent with the results showing that both cortical and thalamic projections to the LAn possess the ability to undergo ITDP, a simultaneous application of ATPA and (S)-DHPG led to potentiation of the EPSC amplitude in thalamic pathway as well (Supplementary Fig. 8a).

We also tested a possibility that the ATPA and (S)-DHPG-evoked potentiation of synaptic transmission in cortical input and ITDP, induced by electrical stimulation with the TSt-CSt pairing protocol, might occlude each other. In these experiments, we used the nystatin-based perforated patch-clamp technique minimizing the effects of postsynaptic “washout” on the induction of synaptic plasticity. Under these conditions, the delivery of the TSt-CSt pairing protocol resulted in gradual potentiation of the EPSC amplitude, reaching the steady-state level within 20 minutes after the induction (Fig. 4e,f). Subsequent simultaneous application of ATPA (1  $\mu$ M) and (S)-DHPG (10  $\mu$ M) for 10 min did not lead to further increases in the EPSC amplitude (Fig. 4e,f), whereas their joint application without the preceding TSt-CSt pairing induced synaptic potentiation (Fig. 4c,d). Importantly, the agonist-induced synaptic potentiation without the prior induction of ITDP could be observed at later times during prolonged perforated patch-clamp recordings (Supplementary Fig. 8b,c). When the order of treatments was reversed, potentiation of the cortico-amygdala EPSC, induced by coapplication of ATPA and DHPG for 10 min, occluded ITDP in response to the standard ITDP-inducing TSt-CSt stimulation (Fig. 4g,h; *t* test,  $P = 0.55$  for the EPSC amplitudes at points (2) and (3) in Fig. 4g). The mutual occlusion of the agonist-induced synaptic potentiation and ITDP indicates that they may be mechanistically similar, providing further support to the notion that activation of GluR5 KARs and group I mGluRs is required for the induction of ITDP in the LAn.

### KARs mediate spatiotemporal summation of convergent inputs

We found that bath application of the GluR5 subunit-specific KAR agonist ATPA (0.1  $\mu$ M – 10  $\mu$ M) both with and without 10 mM BAPTA in pipette solution had no effect on the magnitude of paired-pulse facilitation (PPF, an index of presynaptic function<sup>12</sup>), (Supplementary Fig. 9a–d). This observation indicates that glutamate release is not directly regulated through activation of the GluR5 subunit-containing KARs on cortical terminals in the LAn. The joint application of ATPA and the group I mGluR agonist, (S)-DHPG, resulted in synaptic potentiation in cortico-amygdala pathway (Fig. 4c,d), thus providing evidence that ATPA in a concentration used (1  $\mu$ M) was functionally active. Taken together, these results suggest that GluR5 KARs, implicated in the induction of ITDP, do not directly control presynaptic function in the cortico-LAn projections and are likely to be expressed postsynaptically.

To evaluate a fractional contribution of postsynaptic KARs to the compound cortico-LAn and thalamo-LAn EPSCs, we recorded synaptic responses in the presence of D-AP5 (50  $\mu$ M; EPSC<sub>D-AP5</sub>), and then after an addition to the external solution of the AMPA receptor (AMPA) antagonist SYM 2206 (100  $\mu$ M, EPSC<sub>SYM2206</sub>)<sup>39</sup>. It was followed by application of NBQX (10  $\mu$ M, EPSC<sub>NBQX</sub>), inhibiting both AMPARs and KARs (Fig. 5a). The KAR-mediated EPSC was isolated by subtracting EPSC<sub>NBQX</sub> from EPSC<sub>SYM2206</sub>, while the AMPAR-mediated EPSC was isolated by subtracting EPSC<sub>SYM2206</sub> from EPSC<sub>D-AP5</sub>. Using this approach, we found that  $24\% \pm 2\%$  ( $n = 10$ ) and  $22\% \pm 2\%$  ( $n = 9$ ) of the compound EPSC amplitude were mediated by KARs in cortical and thalamic inputs, respectively (Fig. 5b; no significant difference between inputs,  $P = 0.87$  for AMPAR EPSC;  $P = 0.64$  for KAR-EPSC; *t* test). Consistent with these findings, bath application of the selective antagonist of GluR5 subunit-containing KARs UBP 302 (10  $\mu$ M) resulted in a

decrease of the EPSC amplitude in both cortical and thalamic inputs to  $79\% \pm 3\%$  ( $n = 6$ ,  $P < 0.001$ ) and  $77\% \pm 1\%$  ( $n = 6$ ,  $P < 0.001$ ) of the baseline value, respectively (Supplementary Fig. 10a,b). UBP 302 in this concentration, however, had no effect on PPF in either pathway (Supplementary Fig. 10c), suggesting that the reductions in the EPSC amplitude by UBP 302 were not due to its presynaptic actions. Interestingly, a fractional contribution of the GluR5-KAR-mediated component was unchanged after the induction of ITDP (Supplementary Fig. 10d), indicating that different components of the postsynaptic response were increased proportionally at potentiated synapses. In agreement with the previous studies<sup>40</sup>, the decay time constant of KAR-mediated EPSCs in both inputs was significantly greater than that of AMPAR EPSCs (Fig. 5c,d).

Due to their slow decay kinetics, KAR-mediated EPSCs may display spatiotemporal summation during paired activation of thalamic and cortical afferents with short intervals. To address this possibility, we recorded isolated KAR-mediated EPSCs in the course of paired TSt-CSt stimulation, varying delays between cortical and thalamic stimuli. Indeed, we found that the amplitude of KAR-EPSCs in cortical input was enhanced following priming of thalamic input. Spatiotemporal summation, resulting in the increased amplitude of the KAR-EPSC in cortical input, was maximal at a 15-ms interval between the TSt and CSt (Fig. 5e,f). The EPSC in cortical input, however, displayed significantly reduced spatiotemporal summation when the delay between thalamic and cortical stimuli was 30 ms ( $P < 0.05$  versus the 15-ms interval) or 60 ms ( $P < 0.01$  versus the 15-ms interval). These results could, at least in part, explain the observation that the magnitude of ITDP reached its maximum level at a 15-ms time interval between activation of thalamic and cortical afferent fibers.

### KARs at dendritic spines of LAn neurons are $\text{Ca}^{2+}$ -permeable

The finding that the induction of ITDP in the LAn was dependent on the rise in postsynaptic  $\text{Ca}^{2+}$  concentration, which was not mediated by NMDARs or L-type  $\text{Ca}^{2+}$  channels, while activation of GluR5-containing KARs was required to induce ITDP, suggests that KARs might provide an alternate route of postsynaptic  $\text{Ca}^{2+}$  delivery. It has been established previously that KARs composed of subunits from unedited mRNA at the Q/R site are  $\text{Ca}^{2+}$ -permeable<sup>41</sup> and mediate inwardly rectifying currents when the intracellular solution contains polyamines<sup>42,43</sup>. We therefore examined the current-voltage (I-V) relationship of AMPAR and KAR EPSCs in cortical input to the LAn by recording evoked synaptic responses in a voltage-clamp mode over a range of membrane potentials from  $-70$  to  $+50$  mV. The I-V relation of AMPAR EPSCs (recorded in the presence of D-AP5,  $50 \mu\text{M}$ ) was linear, with a reversal potential  $-0.9 \text{ mV} \pm 0.6 \text{ mV}$  ( $n = 8$ ; Fig. 6a,b). In contrast, the I-V relation of KAR EPSCs (recorded in the presence of D-AP5 and SYM 2206,  $100 \mu\text{M}$ ) exhibited partial inward rectification, as the amplitude of synaptic responses was diminished at  $+30$  mV and  $+50$  mV (Fig. 6a,b). The rectification index, defined as the EPSC amplitude at  $-50$  mV divided by that at  $+50$  mV ( $\text{EPSC}_{-50\text{mV}}/\text{EPSC}_{+50\text{mV}}$ ), was significantly larger for KAR-mediated EPSCs than for AMPAR EPSCs ( $1.44 \pm 0.20$  for KAR EPSCs;  $0.97 \pm 0.05$  for AMPAR EPSCs;  $t$  test,  $P < 0.05$ ). These findings suggest that at least a fraction of KARs activated by stimulation of cortical input might be  $\text{Ca}^{2+}$ -permeable.

We directly tested whether synaptically-activated KARs could mediate  $\text{Ca}^{2+}$  influx at dendritic spines of LAn neurons by visualizing calcium transients in spines with two-photon imaging. We induced  $\text{Ca}^{2+}$  transients using either two-photon photolysis (uncaging) of 4-methoxy-7-nitroindolyl-caged-L-glutamate (MNI-glutamate) or synaptic stimulation. Using whole-cell patch pipettes, we loaded principal neurons with a cytoplasmic dye Alexa 594 (60  $\mu\text{M}$ ) and a  $\text{Ca}^{2+}$  indicator Fluo-5F (300  $\mu\text{M}$ ). The slices were perfused with the external solution containing a low  $\text{Mg}^{2+}$  concentration (0.2 mM), MNI-glutamate (2.5–5 mM) and the antagonist of AMPARs SYM2206 (100  $\mu\text{M}$ ). Glutamate uncaging with the single two-photon laser pulses induced  $\text{Ca}^{2+}$  transients in the dendritic spine (Fig. 6c). The peak amplitudes of  $\text{Ca}^{2+}$  transients, induced by “uncaged” glutamate, were significantly reduced by the selective antagonist of GluR5 subunit-containing KARs UBP 302 (10  $\mu\text{M}$ ;  $n = 8$  spines,  $P < 0.01$ ,  $t$  test; Fig. 6c, right panel). This indicates that the recorded  $\text{Ca}^{2+}$  transients were partly mediated by activation of KARs. The residual  $\text{Ca}^{2+}$  transients recorded in the presence of SYM 2206 and UBP 302 were blocked by D-AP5 (50  $\mu\text{M}$ ), and, therefore, they were mediated by NMDARs (Supplementary Fig. 11a,b).

In a different set of the experiments, we searched for dendritic spines which responded to electrical stimulation of cortical inputs to the LAn. Synaptically-induced  $\text{Ca}^{2+}$  transients were significantly reduced when UBP 302 (10  $\mu\text{M}$ ) was added to the external solution ( $n = 3$  spines,  $P < 0.01$ ,  $t$  test; Fig. 6d). However, activation of KARs by “uncaged” or synaptically-released glutamate, leading to postsynaptic depolarization, could relieve further the voltage-dependent  $\text{Mg}^{2+}$  block, possibly resulting in a component of the spine  $\text{Ca}^{2+}$  influx through NMDAR channels, which would be sensitive to the KAR antagonist. We, therefore, tested the effect of UBP 302 on spine  $\text{Ca}^{2+}$  transients without added  $\text{Mg}^{2+}$  in the external medium when the  $\text{Mg}^{2+}$  block of NMDAR channels is fully relieved. Under these recording conditions, spine  $\text{Ca}^{2+}$  transients, induced by stimulation of cortical input in the presence of the AMPA receptor antagonist SYM 2206 (100  $\mu\text{M}$ ), were still significantly reduced by UBP 302 (10  $\mu\text{M}$ ) (Fig. 6d, right panel;  $n = 3$  spines,  $P < 0.05$ ; paired  $t$  test). Importantly, UBP 302 in this concentration had no direct effect on the amplitude of isolated NMDAR-mediated cortico-LAn EPSCs (Supplementary Fig. 11c,d). Taken together, these findings provide evidence that GluR5 subunit-containing KARs in dendritic spines of LAn neurons are  $\text{Ca}^{2+}$  permeable.

Testing the role of these receptors in the induction process, we found that ITDP was blocked when the TSt-CSt paired stimulation was delivered in the presence of 1-naphthyl acetyl spermine (NASPM, 100  $\mu\text{M}$ ), a synthetic analog of Joro spider toxin (Supplementary Fig. 12c; compare to control ITDP in Supplementary Fig. 7b), known to block  $\text{Ca}^{2+}$ -permeable AMPA/KA receptors<sup>44</sup>. In this concentration, NASPM caused significant reductions in the amplitude of isolated KAR-EPSCs (recorded in the presence of 100  $\mu\text{M}$  SYM 2206), while AMPAR EPSCs (recorded in the presence of 10  $\mu\text{M}$  UBP 302) were not significantly affected (Supplementary Fig. 12a,b). These results provide support to the notion that  $\text{Ca}^{2+}$ -permeable KARs are required for the induction of ITDP in the LAn.

Synaptically-evoked  $\text{Ca}^{2+}$  transients in dendritic spines were only partially blocked by the KAR antagonist while a fraction of the  $\text{Ca}^{2+}$  signal was mediated by activation of NMDARs (Fig. 6d; Supplementary Fig. 11a,b). However, the induction of ITDP in cortical input did

not depend on NMDARs (Fig. 3c,i and Supplementary Fig. 6c,d). To further characterize the conditions underlying ITDP induction, we estimated the magnitudes of the KAR-mediated and NMDAR-mediated EPSPs during delivery of the TSt-CSt stimulation protocol in the current-clamp recording mode in the presence of the physiological concentration of external  $Mg^{2+}$  (1 mM; same concentration of  $Mg^{2+}$  as during the induction of ITDP). EPSPs were evoked by the paired stimulation of thalamic and cortical inputs with a 15-ms interval. Stimulation of cortical input, following activation of the thalamic pathway, resulted in a prominent summation of thalamic and cortical synaptic responses (Fig. 7a). We quantified fractional contributions of the KAR- and NMDAR-mediated components of synaptic responses into the compound EPSP by subtracting traces recorded in the presence of the AMPAR antagonist SYM 2206 (100  $\mu$ M), NBQX (10  $\mu$ M) (Fig. 7a,b) also blocking KARs, and D-AP5 (50 $\mu$ M) (Fig. 7a,b) from baseline responses and from each other (Fig. 7c). We found that nearly 30% of the EPSP, evoked by the TSt-CSt paired stimulation, was mediated by activation of KARs (Fig. 7d) while contribution of the NMDAR-mediated EPSP was small (~10% of a total EPSP amplitude at the resting membrane potential). Similar estimates were obtained in the experiments where the effect of D-APV (50  $\mu$ M) on the EPSP amplitude was tested first (prior to blocking the AMPA/KA receptor component; Supplementary Fig. 13). Evidently, postsynaptic depolarization during the TSt-CSt pairing was insufficient to fully relieve the  $Mg^{2+}$  block of NMDARs, while KARs (which do not require postsynaptic depolarization for their activation) were fully functional under such conditions and could provide  $Ca^{2+}$  required for the induction of ITDP.

### Contribution of ITDP-like mechanisms in fear conditioning

If ITDP, which is sensitive to the blockade of the GluR5 subunit-containing KARs, plays a role in fear conditioning, then inhibition of KA receptors should interfere with the acquisition of conditioned fear memory. Consistent with this prediction, we found that pre-training bilateral intra-amygdala microinfusions of the specific GluR5 subunit-containing KAR antagonist UBP 302 suppressed fear learning. Thus, UBP 302-injected rats froze significantly less at 48 hr post-training in response to the conditioned tone compared to the vehicle-injected animals (Supplementary Fig. 14;  $P < 0.01$  between groups), confirming the role of KAR-dependent processes in the amygdala, such as ITDP, in auditory fear conditioning.

To explore further the role of ITDP in fear conditioning, we tested ITDP in slices from conditioned rats. Memory of fear was assessed by measuring an increase in the freezing response to the tone following fear conditioning (Fig. 8a). Shortly after the fear memory test, we performed whole-cell recordings from neurons in slices from conditioned or control rats. We found that virtually no potentiation could be observed in cortical input to the LAN in slices from conditioned rats (CSa-UCS group) at 35–40 min after the delivery of the TSt-CSt pairing induction protocol ( $t = -15$  ms; Fig. 8b,c;  $t$  test,  $P = 0.18$  versus baseline). However, normal ITDP was observed in slices from behaviorally naïve rats ( $P < 0.001$  versus baseline) or rats which received the CSa only ( $P < 0.05$  versus baseline). These findings demonstrate that ITDP in cortical input to the LAN is occluded following the acquisition of fear memory to the CSa, suggesting that ITDP-like mechanisms may contribute to encoding the fear memory trace.

Using the nystatin-based perforated patch-clamp technique, we also found that the NMDAR-dependent form of LTP, that was induced by pairing presynaptic stimulation at a 2-Hz frequency and postsynaptic depolarization to +30 mV<sup>12</sup>, did not occlude the induction of ITDP (Supplementary Fig. 15). Thus, these two forms of synaptic plasticity at the LAn synapses may contribute to the encoding of conditioned fear memory, synergistically increasing the magnitude of synaptic responses in the CSa pathways during the conditioned stimulus presentation.

## DISCUSSION

Our results demonstrate that continuous low-frequency paired activation of thalamic and cortical auditory inputs with the 15 ms timing delay induces persistent synaptic potentiation at the cortico-amygdala synapses. This induction protocol approximately resembles a temporal pattern of synaptic activation *in vivo*, as a direct thalamic input may deliver the acoustic signals to the LAn ~15–20 ms earlier than an indirect thalamo-cortico-LAn projection<sup>9,24</sup>. The observed form of input timing-dependent plasticity, resulting from associative interactions between two CSa pathways in the LAn, is different from a previously described form of heterosynaptic plasticity which could be triggered in cortical input by subthreshold stimulation of cortical and thalamic afferents with short trains of presynaptic pulses at much higher frequencies (30 Hz) and is induced entirely presynaptically<sup>45</sup>. ITDP is a newly discovered form of synaptic plasticity, which was originally observed in the hippocampus, where pairing of subthreshold stimulation of the distal perforant path-CA1 synapses and the proximal Schaffer collateral-CA1 synapses resulted in potentiation of the Schaffer collateral EPSP, when the inputs were activated at a precise interval<sup>17</sup>.

ITDP in the cortico-LAn projections, explored by us, is mechanistically distinct from a slowly-developing form of heterosynaptic potentiation in inputs to LAn neurons that could be induced by prolonged low-frequency stimulation of cortical fibers alone<sup>35</sup>. ITDP in cortical input to the LAn, that required joint activation of cortical and thalamic afferents for its induction, was pathway-specific at physiological temperatures (not heterosynaptic), suggesting a potential functional role for this newly discovered form of synaptic plasticity in the CSa pathways at the behavioral level. Consistent with this notion, ITDP was occluded in slices from fear-conditioned rats. Moreover, similar to ITDP, the acquisition of fear memory was sensitive to the blockade of the GluR5-containing KARs (but see<sup>40</sup>). These findings indicate that ITDP-like synaptic enhancements in cortical input to the LAn might be recruited during fear conditioning.

Insufficient postsynaptic depolarization during the induction process could explain why ITDP in the LAn, while implicating an increase in the postsynaptic Ca<sup>2+</sup> concentration, does not depend on activation of NMDARs (unlike ITDP in the hippocampus that is NMDAR-dependent<sup>17</sup>) or L-type voltage-gated calcium channels. Ca<sup>2+</sup> release from the InsP<sub>3</sub>-sensitive internal stores, which is possibly mediated by synaptic activation of group I mGluRs, contributes to the rises in a postsynaptic Ca<sup>2+</sup> concentration in LAn neurons during the ITDP-inducing stimulation. Importantly, the acquisition of conditioned fear memory was shown to depend on activation of group I mGluRs in the amygdala<sup>46</sup>. As we demonstrated in

our two-photon imaging and glutamate uncaging studies, GluR5-subunit-containing KARs in the LAN are  $\text{Ca}^{2+}$  permeable, and, therefore, provide a likely route of the postsynaptic  $\text{Ca}^{2+}$  delivery during ITDP induction. Consistent with this notion, approximately 30% of GluR5 mRNA in the amygdala is present in an unedited form<sup>35</sup>. KARs, which are composed of subunits unedited in their Q/R site, display  $\text{Ca}^{2+}$ -permeability, whereas KARs containing subunits from edited mRNA are  $\text{Ca}^{2+}$ -impermeable<sup>41</sup>. ITDP was prevented when either of the inductive calcium signals, the release of  $\text{Ca}^{2+}$  from the internal stores due to activation of group I mGluRs or postsynaptic  $\text{Ca}^{2+}$  influx through calcium-permeable KARs, was suppressed. This could indicate that the threshold intracellular  $\text{Ca}^{2+}$  concentration, required for the induction of ITDP in the LAN, could only be reached when both sources of postsynaptic calcium are simultaneously recruited during the induction process. The mGluR-mediated  $\text{Ca}^{2+}$  release is not time-locked. Therefore the temporal requirements for the induction of ITDP are likely to be mediated by the characteristics of GluR5-KAR-mediated synaptic responses in convergent projections to the LAN. Spatiotemporal summation of the slowly-decaying KAR-mediated EPSCs during paired activation of the thalamic and cortical afferents resulted in the enlargement of the KAR-mediated synaptic responses in cortical input, which was most prominent when the interval between thalamic and cortical signals converging in the LAN was matched to the ~15 ms delay. This finding implies that the cellular machinery involved in the induction of ITDP in the LAN and in maintaining its pathway specificity might be finely tuned to detect temporal patterns of activation in the CSa pathways.

Recent combined electrophysiological and imaging studies provide evidence that cortical and thalamic afferents could converge on the same dendritic branch, forming active synapses on spines which could be as close as less than  $5\ \mu\text{m}$ <sup>47</sup>. Nevertheless, thalamic and cortical inputs function independently under conditions of the low frequency basal presynaptic activity. Pathway specificity of ITDP at the LAN synapses is controlled by active glutamate uptake and is only lost when glutamate transporters are inactivated. Therefore, it is unlikely that the diffusion of glutamate from thalamic to cortical input would contribute to the induction of ITDP. Since ITDP in the LAN requires an increase in postsynaptic  $\text{Ca}^{2+}$  concentration, the interaction between synapses activated by thalamic and cortical fibers is likely to occur within the dendritic branch. A recent study demonstrated that the induction of LTP at an individual synapse could be associated with the reduction of the threshold for LTP induction at neighboring dendritic spines<sup>48</sup>. By analogy, during the induction of ITDP in the LAN, the instructive signal resulting from the priming activation of thalamic input could spread from “thalamic” spines to the closely located spines possessing synapses activated by cortical fibers, thus facilitating the induction of ITDP in cortical pathway.

While the temporal patterns of the signals' flow in the CSa projections during behavioral training might be more complex than that modeled in this study, our results, nevertheless, provide evidence that ITDP might be functionally relevant. The firing rates of neurons in the LAN are notoriously low both under baseline conditions and during the acquisition of fear memory<sup>49</sup>. The levels of presynaptic activity, associated with the CSa presentation, might be insufficient to produce the functionally relevant membrane depolarization in LAN neurons during behavioral training. ITDP, possibly acting in concert with the conventional NMDAR-

dependent forms of synaptic plasticity (which result from the CSa-UCS pairing and also contribute to the acquisition of fear memory<sup>12,34</sup>), could provide an additional mechanism of synaptic strengthening in the CSa pathways that is nearly entirely determined by the spatiotemporal characteristics of the convergent presynaptic activity patterns.

## METHODS

Methods and any associated references are available in the online version of the paper at <http://www.nature.com/natureneuroscience/>

## Supplementary Material

Refer to Web version on PubMed Central for supplementary material.

## Acknowledgments

We thank Yan Li and Keith Tully for constructive discussions. This study was supported by NIH grants MH083011 (V.Y.B.), MH090464 (V.Y.B.) and MH079079 (S.S.Z.), the National Alliance for Research on Schizophrenia and Depression (V.Y.B.), Whitehall Foundation (V.Y.B.), and USAMRAA Grant #W81XWH-08-2-0126 (to V.Y.B.).

## References

1. LeDoux JE. Emotion circuits in the brain. *Annu Rev Neurosci.* 2000; 23:155–184. [PubMed: 10845062]
2. Maren S, Quirk GJ. Neuronal signalling of fear memory. *Nat Rev Neurosci.* 2004; 5:844–852. [PubMed: 15496862]
3. Romanski LM, LeDoux JE. Equipotentiality of thalamo-amygdala and thalamo-cortico-amygdala circuits in auditory fear conditioning. *J Neurosci.* 1992; 12:4501–4509. [PubMed: 1331362]
4. Campeau S, Davis M. Involvement of subcortical and cortical afferents to the lateral nucleus of the amygdala in fear conditioning measured with fear-potentiated startle in rats trained concurrently with auditory and visual conditioned stimuli. *J Neurosci.* 1995; 15:2312–2327. [PubMed: 7891169]
5. Armony JL, Servan-Schreiber D, Romanski LM, Cohen JD, LeDoux JE. Stimulus generalization of fear responses: effects of auditory cortex lesions in a computational model and in rats. *Cereb Cortex.* 1997; 7:157–165. [PubMed: 9087823]
6. Clugnet MC, LeDoux JE. Synaptic plasticity in fear conditioning circuits: induction of LTP in the lateral nucleus of the amygdala by stimulation of the medial geniculate body. *J Neurosci.* 1990; 10:2818–24. [PubMed: 2388089]
7. Bordi F, LeDoux JE. Response properties of single units in areas of rat auditory thalamus that project to the amygdala. II. Cells receiving convergent auditory and somatosensory inputs and cells antidromically activated by amygdala stimulation. *Exp Brain Res.* 1994; 98:275–286. [PubMed: 8050513]
8. Quirk GJ, Reppas CB, LeDoux JE. Fear conditioning enhances short-latency auditory responses of lateral amygdala neurons: Parallel recordings in the freely behaving rat. *Neuron.* 1995; 15:1029–1039. [PubMed: 7576647]
9. Quirk GJ, Armony JL, LeDoux JE. Fear conditioning enhances different temporal components of tone-evoked spike trains in auditory cortex and lateral amygdala. *Neuron.* 1997; 19:613–624. [PubMed: 9331352]
10. Rogan MT, Staubli UV, LeDoux JE. Fear conditioning induces associative long-term potentiation in the amygdala. *Nature.* 1997; 390:604–607. [PubMed: 9403688]
11. McKernan MG, Shinnick-Gallagher P. Fear conditioning induces a lasting potentiation of synaptic currents in vitro. *Nature.* 1997; 390:607–611. [PubMed: 9403689]

12. Tsvetkov E, Carlezon WA, Benes FM, Kandel ER, Bolshakov VY. Fear conditioning occludes LTP-induced presynaptic enhancement of synaptic transmission in the cortical pathway to the lateral amygdala. *Neuron*. 2002; 34:289–300. [PubMed: 11970870]
13. Rumpel S, LeDoux J, Zador A, Malinow R. Postsynaptic receptor trafficking underlying a form of associative learning. *Science*. 2005; 308:83–88. [PubMed: 15746389]
14. Shumyatsky GP, et al. *Stathmin*, a gene enriched in the amygdala, controls both learned and innate fear. *Cell*. 2005; 123:697–709. [PubMed: 16286011]
15. Tsvetkov E, Shin RM, Bolshakov VY. Glutamate uptake determines pathway specificity of long-term potentiation in the neural circuitry of fear conditioning. *Neuron*. 2004; 41:139–151. [PubMed: 14715141]
16. Doyere V, Schafe GE, Sigurdsson T, LeDoux JE. Long-term potentiation in freely moving rats reveals asymmetries in thalamic and cortical inputs to the lateral amygdala. *Eur J Neurosci*. 2003; 17:2703–2715. [PubMed: 12823477]
17. Dudman JT, Tsay D, Siegelbaum SA. A role for synaptic inputs at distal dendrites: instructive signals for hippocampal long-term plasticity. *Neuron*. 2007; 56:866–879. [PubMed: 18054862]
18. Mahanty NK, Sah P. Calcium-permeable AMPA receptors mediate long-term potentiation in interneurons in the amygdala. *Nature*. 1998; 394:683–687. [PubMed: 9716132]
19. LeDoux JE, Ruggiero DA, Reis DJ. Projections to the subcortical forebrain from anatomically defined regions of the medial geniculate body in the rat. *J Comp Neurol*. 1985; 242:182–213. [PubMed: 4086664]
20. Mascagni F, McDonald AJ, Coleman JR. Corticoamygdaloid and corticocortical projections of the rat temporal cortex: a Phaseolus vulgaris leucoagglutinin study. *Neuroscience*. 1993; 57:697–715. [PubMed: 8309532]
21. Romanski LM, LeDoux JE. Information cascade from primary auditory cortex to the amygdala: corticocortical and corticoamygdaloid projections of temporal cortex in the rat. *Cereb Cortex*. 1993; 3:515–532. [PubMed: 7511012]
22. Shin RM, Tsvetkov E, Bolshakov VY. Spatiotemporal asymmetry of associative synaptic plasticity in fear conditioning pathways. *Neuron*. 2006; 52:883–896. [PubMed: 17145508]
23. Shin RM, et al. Hierarchical order of coexisting pre- and postsynaptic forms of long-term potentiation at synapses in amygdala. *Proc Natl Acad Sci USA*. 2010; 107:19073–19078. [PubMed: 20956319]
24. Li XF, Stutzmann GE, LeDoux JE. Convergent but temporally separated inputs to lateral amygdala neurons from the auditory thalamus and auditory cortex use different postsynaptic receptors: in vivo intracellular and extracellular recordings in fear conditioning pathways. *Learn Mem*. 1996; 3:229–242. [PubMed: 10456093]
25. Johnson LR, et al. A recurrent network in the lateral amygdala: a mechanism for coincidence detection. *Front Neural Circuits*. 2008; 2:3.10.3389/neuro.04.003.2008 [PubMed: 19104668]
26. Sugita S, Tanaka E, North RA. Membrane properties and synaptic potentials of three types of neurone in rat lateral amygdala. *J Physiol*. 1993; 460:705–718. [PubMed: 8487215]
27. Li XF, Armony JL, LeDoux JE. GABAA and GABAB receptors differentially regulate synaptic transmission in the auditory thalamo-amygdala pathway: an in vivo microiontophoretic study and a model. *Synapse*. 1996; 24:115–124. [PubMed: 8890453]
28. Lang EJ, Paré D. Similar inhibitory processes dominate the responses of cat lateral amygdaloid projection neurons to their various afferents. *J Neurophysiol*. 1997; 77:341–352. [PubMed: 9120575]
29. Bissiere S, Humeau Y, Luthi A. Dopamine gates LTP induction in lateral amygdala by suppressing feedforward inhibition. *Nat Neurosci*. 2003; 6:587–592. [PubMed: 12740581]
30. Kodirov SA, et al. Synaptically released zinc gates long-term-potentiation in fear conditioning pathways. *Proc Natl Acad Sci USA*. 2006; 103:15218–15223. [PubMed: 17005717]
31. Tully K, Li Y, Tsvetkov E, Bolshakov VY. Norepinephrine enables the induction of associative long-term potentiation at thalamo-amygdala synapses. *Proc Natl Acad Sci USA*. 2007; 104:14146–14150. [PubMed: 17709755]

32. Asztely F, Erdemli G, Kullmann DM. Extrasynaptic glutamate spillover in the hippocampus: dependence on temperature and the role of active glutamate uptake. *Neuron*. 1997; 18:281–293. [PubMed: 9052798]
33. Huang YY, Kandel ER. Postsynaptic induction and PKA-dependent expression of LTP in the lateral amygdala. *Neuron*. 1998; 21:169–178. [PubMed: 9697861]
34. Bauer EP, Schafe GE, LeDoux JE. NMDA receptors and L-type voltage-gated calcium channels contribute to long-term potentiation and different components of fear memory formation in the lateral amygdala. *J Neurosci*. 2002; 22:5239–5249. [PubMed: 12077219]
35. Li H, Chen A, Xing G, Wei ML, Rogawski MA. Kainate receptor-mediated heterosynaptic facilitation in the amygdala. *Nat Neurosci*. 2001; 4:612–620. [PubMed: 11369942]
36. Bortolotto ZA, et al. Kainate receptors are involved in synaptic plasticity. *Nature*. 1999; 402:297–301. [PubMed: 10580501]
37. Raymond CR, Redman SJ. Different calcium sources are narrowly tuned to the induction of different forms of LTP. *J Neurophysiol*. 2002; 88:249–255. [PubMed: 12091550]
38. Bardo S, Cavazzini MG, Emptage N. The role of the endoplasmic reticulum Ca<sup>2+</sup> store in the plasticity of central neurons. *Trends Pharmacol Sci*. 2006; 27:78–84. [PubMed: 16412523]
39. Li P, et al. Kainate-receptor-mediated sensory synaptic transmission in mammalian spinal cord. *Nature*. 1999; 397:161–164. [PubMed: 9923678]
40. Ko S, Zhao MG, Toyoda H, Qiu CS, Zhuo M. Altered behavioral responses to noxious stimuli and fear in glutamate receptor 5 (GluR5)- or GluR6-deficient mice. *J Neurosci*. 2005; 25:977–984. [PubMed: 15673679]
41. Burnashev N, Villarroel A, Sakmann B. Dimensions and ion selectivity of recombinant AMPA and kainate receptor channels and their dependence on Q/R site residues. *J Physiol*. 1996; 496:165–173. [PubMed: 8910205]
42. Bowie D, Mayer ML. Inward rectification of both AMPA and kainate subtype glutamate receptors generated by polyamine-mediated ion channel block. *Neuron*. 1995; 15:453–462. [PubMed: 7646897]
43. Wilding TJ, Zhou Y, Huettner JE. Q/R site editing controls kainate receptor inhibition by membrane fatty acids. *J Neurosci*. 2005; 25:9470–9478. [PubMed: 16221857]
44. Koike M, Iino M, Ozawa S. Blocking effect of 1-naphthyl acetyl spermine on Ca(2+)-permeable AMPA receptors in cultured rat hippocampal neurons. *Neurosci Res*. 1997; 29:27–36. [PubMed: 9293490]
45. Humeau Y, Shaban H, Bissiere S, Luthi A. Presynaptic induction of heterosynaptic associative plasticity in the mammalian brain. *Nature*. 2003; 426:841–845. [PubMed: 14685239]
46. Rodrigues SM, Bauer EP, Farb CR, Schafe GE, LeDoux JE. The group I metabotropic glutamate receptor mGluR5 is required for fear memory formation and long-term potentiation in the lateral amygdala. *J Neurosci*. 2002; 22:5219–5229. [PubMed: 12077217]
47. Humeau Y, et al. Dendritic spine heterogeneity determines afferent-specific Hebbian plasticity in the amygdala. *Neuron*. 2005; 45:119–131. [PubMed: 15629707]
48. Harvey CD, Svoboda K. Locally dynamic synaptic learning rules in pyramidal neuron dendrites. *Nature*. 2007; 450:1195–1200. [PubMed: 18097401]
49. Pare D, Collins DR. Neuronal correlates of fear in the lateral amygdala: multiple extracellular recordings in conscious cats. *J Neurosci*. 2000; 20:2701–2710. [PubMed: 10729351]
50. Richardson RJ, Blundon JA, Bayazitov IT, Zakharenko SS. Connectivity patterns revealed by mapping of active inputs on dendrites of thalamorecipient neurons in the auditory cortex. *J Neurosci*. 2009; 29:6406–6417. [PubMed: 19458212]

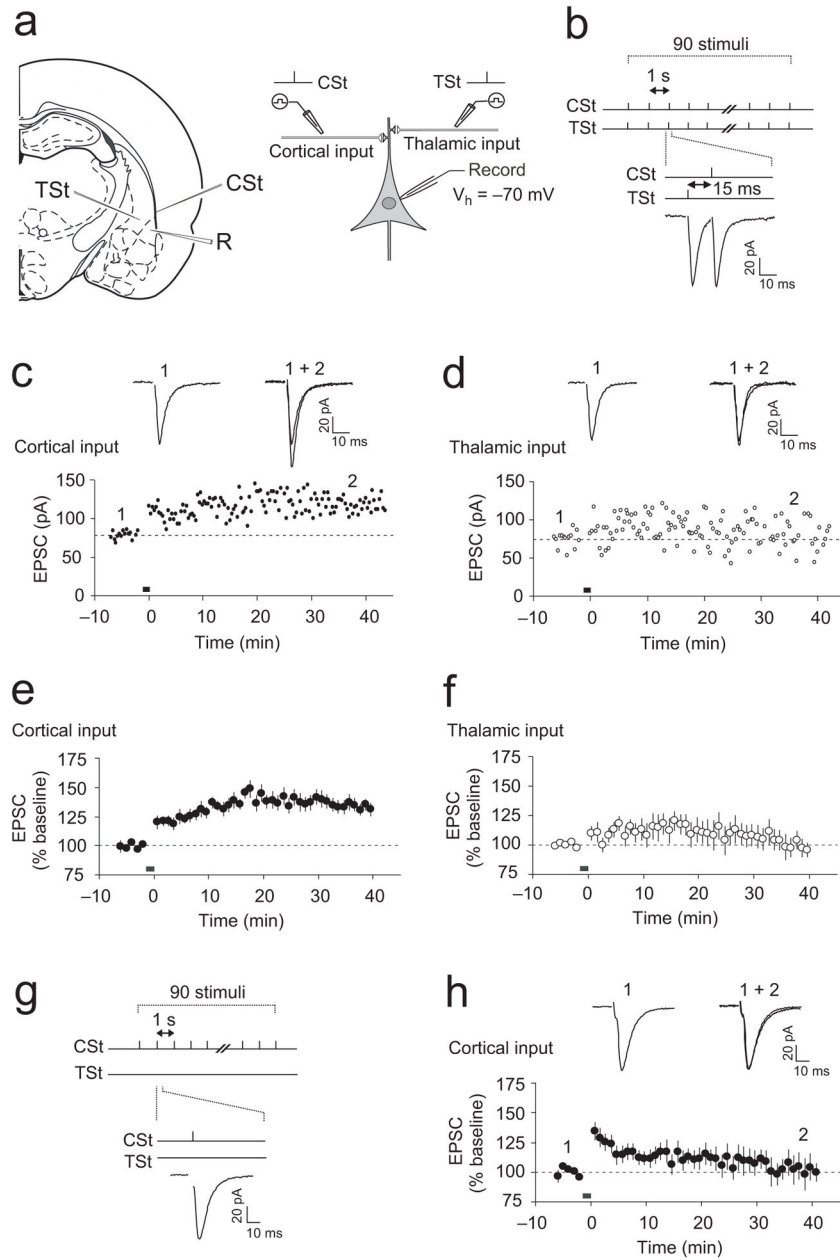


**Figure 1.** Paired stimulation of thalamic and cortical inputs induces ITDP at the cortico-LAN synapses. (a) Schematic representations of the slice preparation, showing positions of recording and stimulation electrodes (left), and the experimental design (right). Stimulation electrodes (CSt and TSt) were positioned to activate cortical or thalamic inputs, respectively. R, recording electrode. (b) A diagram illustrating the TSt-CSt protocol, consisting of paired stimulation of thalamic and cortical inputs. TSt was delivered 15 ms earlier than CSt. Below, examples of the EPSCs during the TSt-CSt stimulation. (c) TSt-CSt pairing-induced ITDP in cortical input to the LAN. Insets show the average of fifteen cortico-LAN EPSCs recorded before (1) and 35–40 min after (2) the TSt-CSt stimulation (black horizontal bar). Stimulation artifacts

were removed for clarity in these and all other examples of EPSCs. **(d)** EPSCs in thalamic input in the same experiment as in **(c)**. Insets show the average of fifteen thalamo-LAn EPSCs before (1) and after (2) the TSt-CSt stimulation. **(e)** Summary graph of all experiments as in **(c)** ( $n = 13$ , paired  $t$  test,  $P < 0.001$  versus baseline). The magnitude of potentiation was determined at 35–40 min after the induction. **(f)** Summary graph of all experiments as in **(d)** ( $n = 11$ ,  $P = 0.53$  versus baseline). **(g)** Design of experiments where TSt was omitted. **(h)** Potentiation of cortico-LAn EPSCs was not observed if only cortical input was stimulated (black bar) ( $n = 6$ ,  $P = 0.55$  versus baseline). Error bars indicate s.e.m.

Author Manuscript

Author Manuscript

Author Manuscript

Author Manuscript

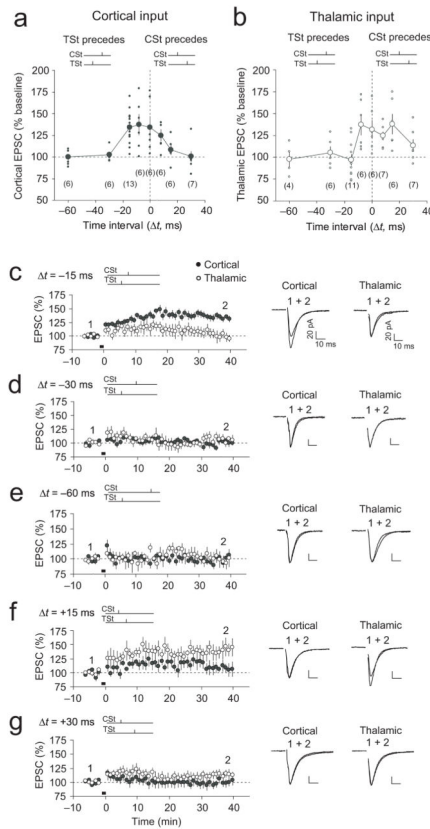


**Figure 2.**

Dependence of ITDP induction on time interval between TSt and CSt. **(a)** Normalized amplitude (% baseline) of the cortico-LAn EPSC at 35–40 min after paired stimulation when either the TSt preceded the CSt ( $-t$ ) or the CSt preceded the TSt ( $+t$ ). Time intervals during TSt-CSt pairing (in ms): 0,  $-8$ ,  $-15$ ,  $-30$  and  $-60$ ; during CSt-TSt pairing:  $+8$ ,  $+15$  and  $+30$ . Data points represent individual experiments. The number of experiments is indicated in brackets. **(b)** Amplitude of the thalamo-LAn EPSC after paired stimulation (same experimental design as in **(a)**). **(c)** Summary graph demonstrating the time course of EPSC amplitude changes before and after TSt-CSt stimulation with  $t = -15$  ms. Same data as in Fig. 1e,f were included here for a comparison with other  $t$ . Traces are averages of fifteen EPSCs recorded before (1) and after (2) the coactivation (black bar). **(d)** Same as in **(c)** but with  $t = -30$  ms ( $n = 6$ , paired  $t$  test,  $P = 0.50$  versus baseline in cortical input). **(e)** Same as in **(c)** and **(d)** but with  $t = -60$  ms ( $n = 6$ ,  $P = 0.94$  versus baseline in cortical input). **(f)** Summary of experiments with  $t = +15$  ms during the CSt-TSt pairing ( $n = 6$ ,  $P < 0.05$  versus baseline in thalamic input, but  $P = 0.27$  versus baseline in cortical input). **(g)** Same as in **(f)** but with  $t = +30$  ms ( $n = 7$ ). Scale bars: 20 pA, 10 ms. Error bars indicate s.e.m.

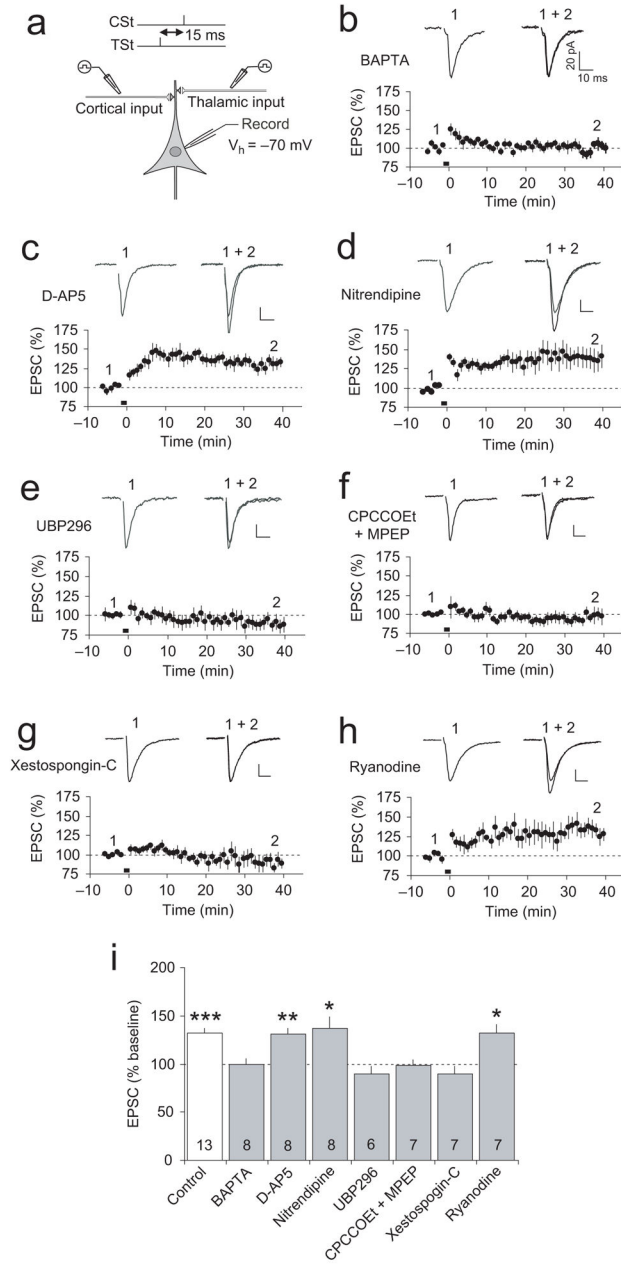


**Figure 3.** Requirements for the induction of ITDP. **(a)** Experimental design. **(b)** ITDP in cortical input was blocked by BAPTA (10 mM) in the recording pipette solution ( $n = 8$ , paired  $t$  test,  $P = 0.67$  versus baseline). Insets show the average of fifteen cortico-LAN EPSCs before (1) and after (2) the TSt-CSSt stimulation. Scale bars here and for other traces in the figure: 20 pA and 10 ms. **(c)** ITDP in cortical input in the presence of D-AP5 (50  $\mu$ M,  $n = 8$ ,  $P < 0.01$  versus baseline). **(d)** ITDP in cortical input in the presence of nitrendipine (20  $\mu$ M,  $n = 8$ ,  $P < 0.05$  versus baseline). **(e)** ITDP in cortical input was blocked in the presence of UBP 296 (5  $\mu$ M,  $n = 6$ ,  $P = 0.23$  versus baseline). **(f)** Joint application of CPCCOEt (40  $\mu$ M) and MPEP (20  $\mu$ M) also blocked ITDP ( $n = 7$ ,  $P = 0.61$  versus baseline). **(g)** Xestospongine-C (10

$\mu\text{M}$ ) in pipette solution blocked the induction of ITDP ( $n = 7$ ,  $P = 0.39$  versus baseline). **(h)** Inclusion of ryanodine ( $100 \mu\text{M}$ ) in pipette solution had no effect on ITDP ( $n = 7$ ,  $P < 0.05$  versus baseline). **(i)** Summary of ITDP experiments. Numbers within bars indicate the number of experiments for each condition.  $*P < 0.05$ ,  $**P < 0.01$ , and  $***P < 0.001$ , mean baseline EPSC amplitude versus EPSCs recorded 35–40 minutes after the TSt-CSt pairing, paired  $t$  test. Error bars indicate s.e.m.

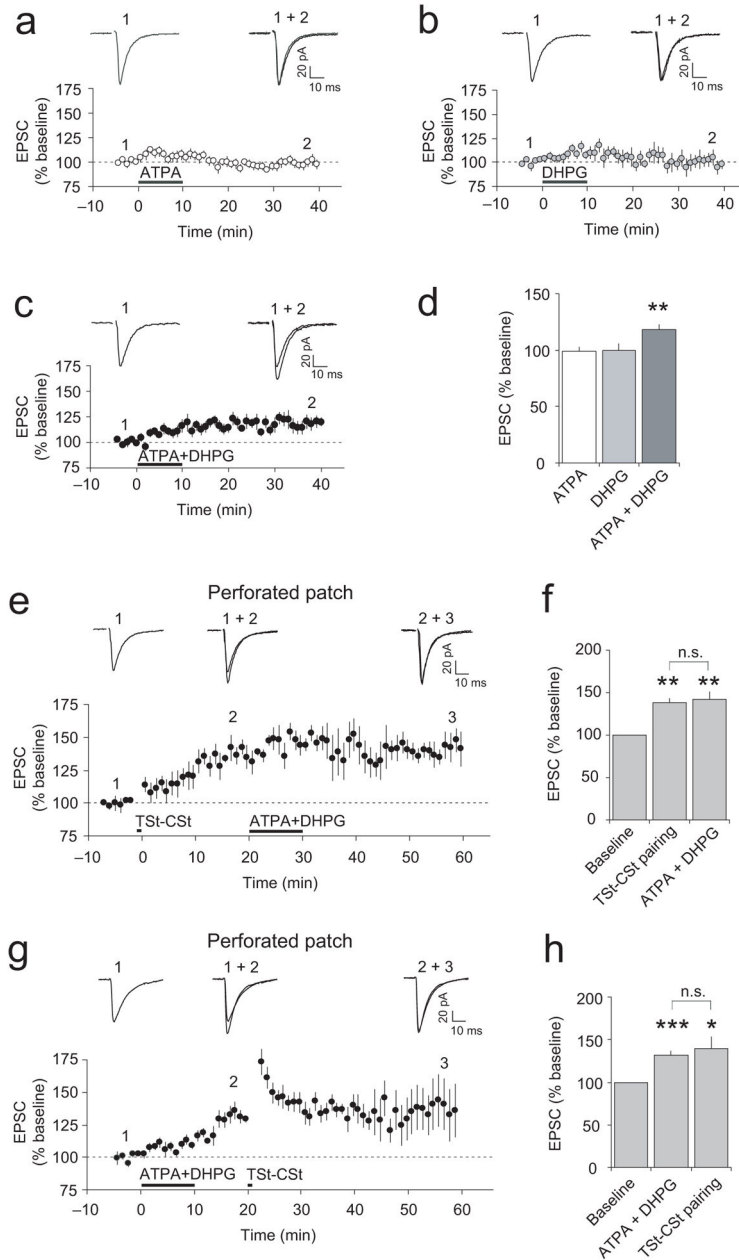


**Figure 4.** Coactivation of GluR5-containing KARs and group I mGluRs during ITDP induction. (a and b) Application of ATPA (1  $\mu$ M) or (S)-DHPG (10  $\mu$ M) alone did not potentiate the cortico-LAN EPSCs (ATPA:  $n = 10$ ,  $P = 0.76$  versus baseline; (S)-DHPG:  $n = 6$ ,  $P = 0.95$ ; paired  $t$  test). Insets show averaged cortico-LAN EPSCs recorded before (1) and at the end (2) of ATPA or (S)-DHPG application. (c) Applied jointly, ATPA and (S)-DHPG induced potentiation of the EPSC in cortical input ( $n = 8$ ). (d) Summary of the ATPA and (S)-DHPG effects on cortico-LAN EPSCs (\*\* $P < 0.01$  versus baseline). (e) Perforated patch technique was used in these experiments. The induction of ITDP (TSt-CSt pairing,  $t = -15$  ms) occluded potentiation of the EPSC by jointly-applied ATPA and (S)-DHPG ( $n = 5$ ). (f)

Summary of the experiments as in (e). Jointly-applied ATPA and (S)-DHPG did not produce additional potentiation in cortical input ( $n = 5$ , paired  $t$  test,  $P = 0.49$  for ITDP magnitude versus potentiation with subsequently-added agonists, n.s.).  $**P < 0.01$  for both ITDP magnitude and potentiation after addition of agonists versus the baseline. (g) The order of treatments was reversed. Coapplication of ATPA and (S)-DHPG preceded TSt-CSt stimulation ( $n = 7$ ). (h) Summary of the experiments as in (g):  $***P < 0.001$  for agonist-induced potentiation and  $*P < 0.05$  for the EPSC amplitude following TSt-CSt stimulation versus the baseline EPSC; no significant difference for agonist-induced potentiation versus ITDP magnitude,  $P = 0.55$ . Error bars indicate s.e.m.

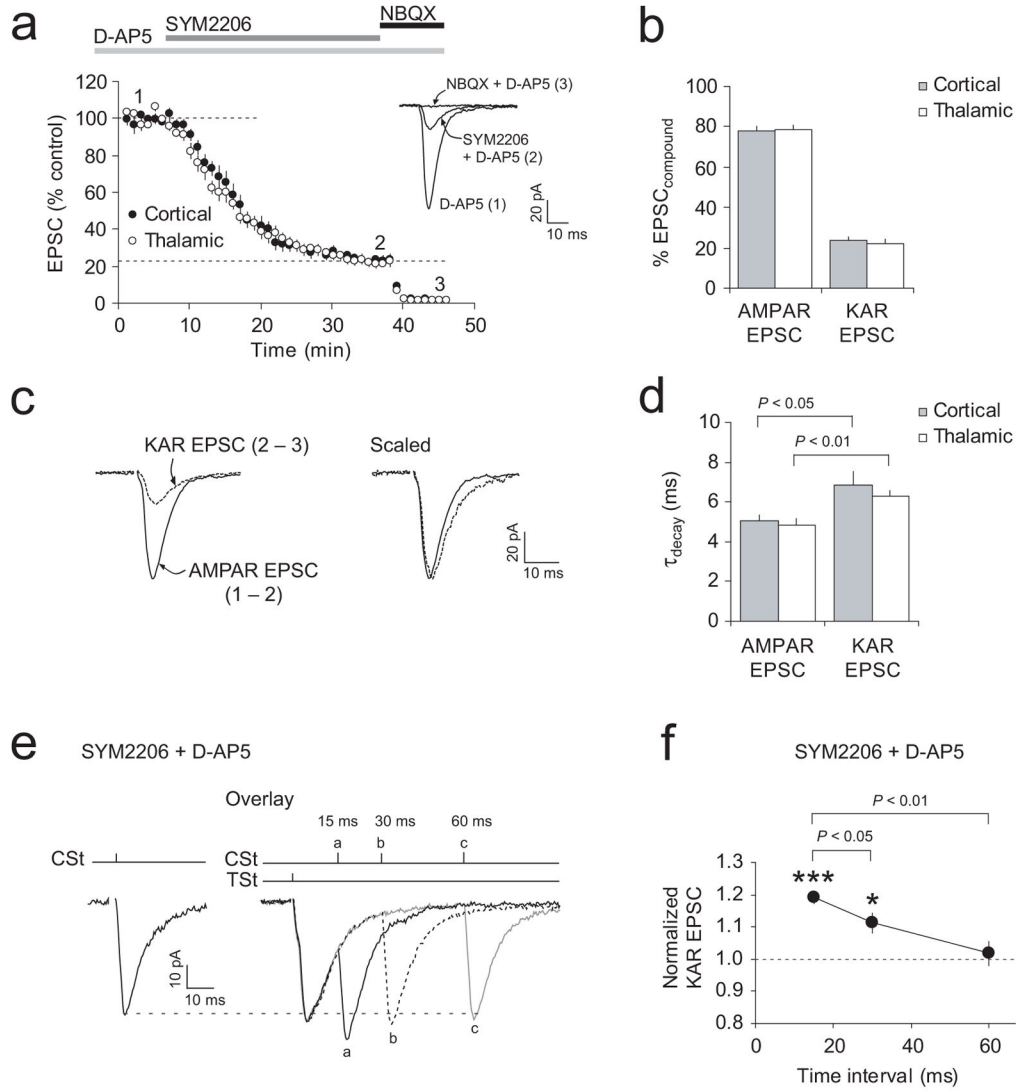


**Figure 5.** Spatiotemporal summation of KAR-mediated EPSCs during TSt-CSSt stimulation. **(a)** Effects of SYM 2206 (100  $\mu$ M) and NBQX (10  $\mu$ M) on the EPSC amplitude in cortical ( $n = 10$ ) and thalamic ( $n = 9$ ) inputs in the presence of D-AP5 (50 $\mu$ M). Inset shows the averages of fifteen traces under baseline conditions (1), during SYM 2206-induced depression (2), and after NBQX addition (3). **(b)** Fractional contribution of the AMPAR- and KAR-mediated current components. To isolate the KAR-mediated EPSC, EPSC<sub>NBQX</sub> (trace 3 in **a**) was subtracted from EPSC<sub>SYM2206</sub> (trace 2). The AMPAR-mediated EPSC was isolated by subtracting EPSC<sub>SYM2206</sub> (trace 2) from EPSC<sub>D-AP5</sub> (trace 1). **(c)** Left, examples of isolated AMPAR- and KAR-mediated EPSCs. Right, same traces scaled by their peak amplitudes. **(d)** Decay time constants (from a single-exponential fit) of AMPAR-EPSCs and KAR-EPSCs in cortical ( $n = 8$ ) and thalamic ( $n = 8$ ) inputs. KAR-mediated EPSCs decayed significantly slower ( $P < 0.05$  for cortical input,  $P < 0.01$  for thalamic input, paired  $t$  test). **(e)** Left, KAR-mediated EPSC when cortical input was stimulated alone. Right, KAR-EPSCs when TSt preceded CSt by 15 ms (a), 30 ms (b), and 60 ms (c). **(f)** Spatiotemporal summation of

KAR-mediated EPSCs depended on the time interval between TSt and CSt during paired stimulation. EPSCs were normalized to the EPSC evoked by CSt alone ( $n = 7$ ,  $*P < 0.05$  for 30-ms delay, and  $***P < 0.001$  for 15 ms-delay during the TSt-CSt pairing versus CSt alone; paired  $t$  test). Error bars indicate s.e.m.

Author Manuscript

Author Manuscript

Author Manuscript

Author Manuscript

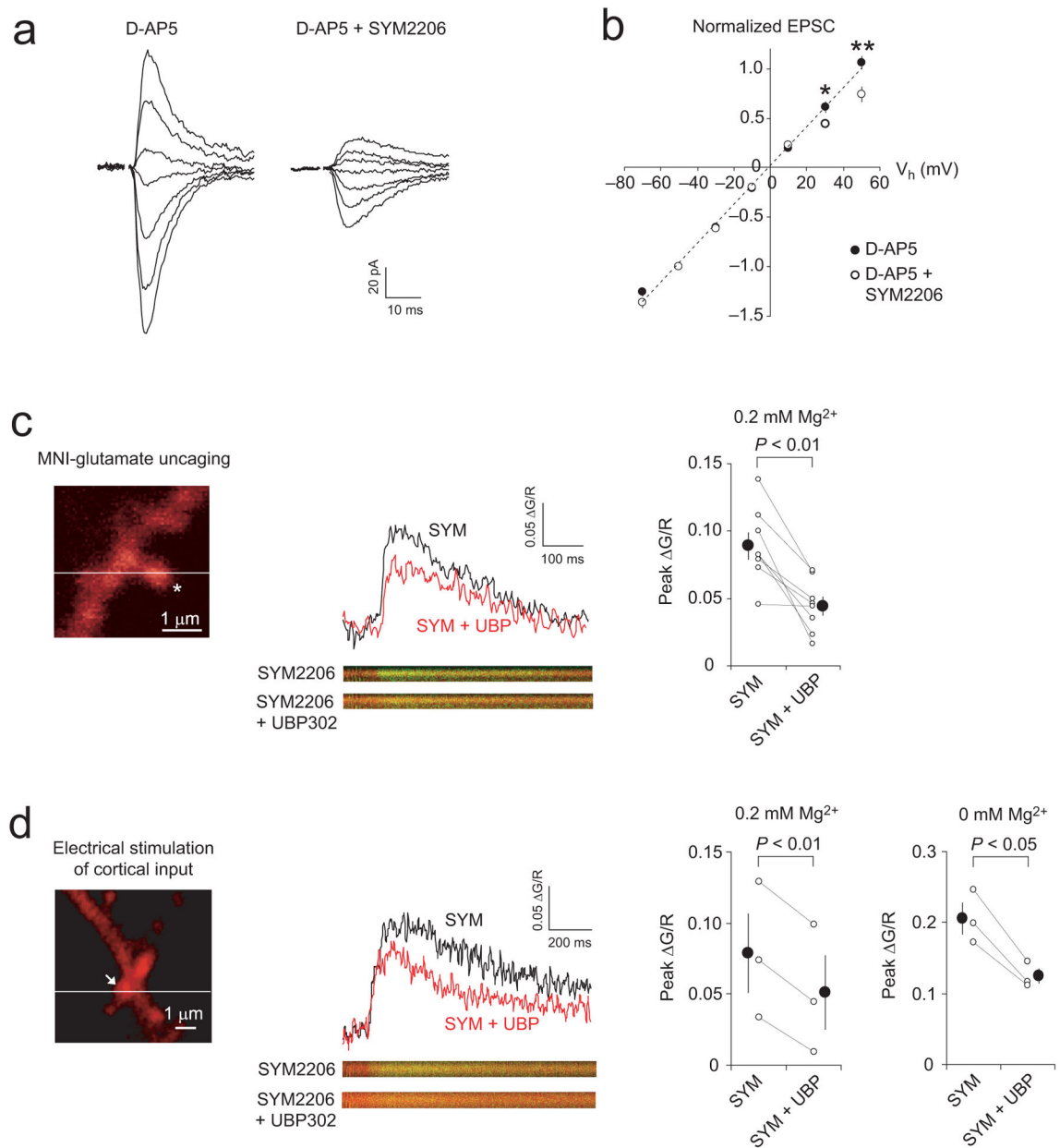


**Figure 6.**

KARs in dendritic spines of LAn neurons are  $\text{Ca}^{2+}$ -permeable (a) EPSCs in cortical input at holding potentials from  $-70$  mV to  $+50$  mV in the presence of D-AP5 ( $50 \mu\text{M}$ ) or D-AP5 + SYM 2206 ( $100 \mu\text{M}$ ). (b) I-V plots of the cortico-LAn EPSCs ( $n = 8$ ). The peak EPSC amplitude at each holding potential was normalized to the amplitude at  $-50$  mV. The I-V plot became inwardly-rectifying when SYM 2206 was added ( $*P < 0.05$ ,  $**P < 0.01$ ;  $t$  test). (c) Left, the two-photon microscopic image of dendritic spine of LAn neuron. Asterisk, the position of uncaging laser pulse. Horizontal line, the position of line scans. Middle,  $\text{Ca}^{2+}$  transients were evoked by uncaging MNI-glutamate ( $2.5$ – $5$  mM) with single two-photon laser pulses in the presence of  $0.2$  mM  $\text{Mg}^{2+}$  and  $100 \mu\text{M}$  SYM 2206.  $\text{Ca}^{2+}$  transients were quantified as the ratio of change in green ( $\text{Ca}^{2+}$ -sensitive dye, Fluo-5F) to red (structural

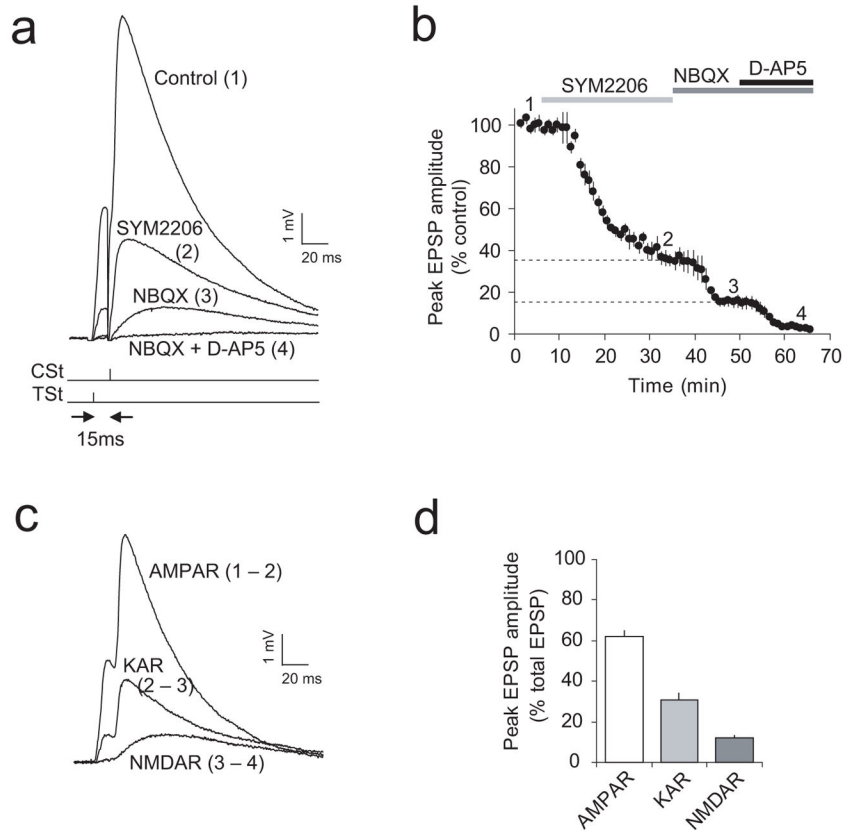
dye, Alexa 594) fluorescence (  $G/R$ ). The  $Ca^{2+}$  transient was reduced by UBP 302 (10  $\mu M$ ). Right, summary of the UBP 302 effects on  $Ca^{2+}$  transients (8 dendritic spines). **(d)** Left, dendritic spine (arrow) which was stimulated with electrical pulses delivered to cortical input in the presence of 0.2 mM  $Mg^{2+}$  and SYM 2206. Middle, UBP 302 reduced synaptically-induced  $Ca^{2+}$  transients in dendritic spine. Right, summary of UBP 302-induced changes in synaptically-induced  $Ca^{2+}$  transients when external solution contained either 0.2 mM  $Mg^{2+}$  (3 experiments) or 0 mM  $Mg^{2+}$  (3 experiments). Error bars indicate s.e.m.

Author Manuscript

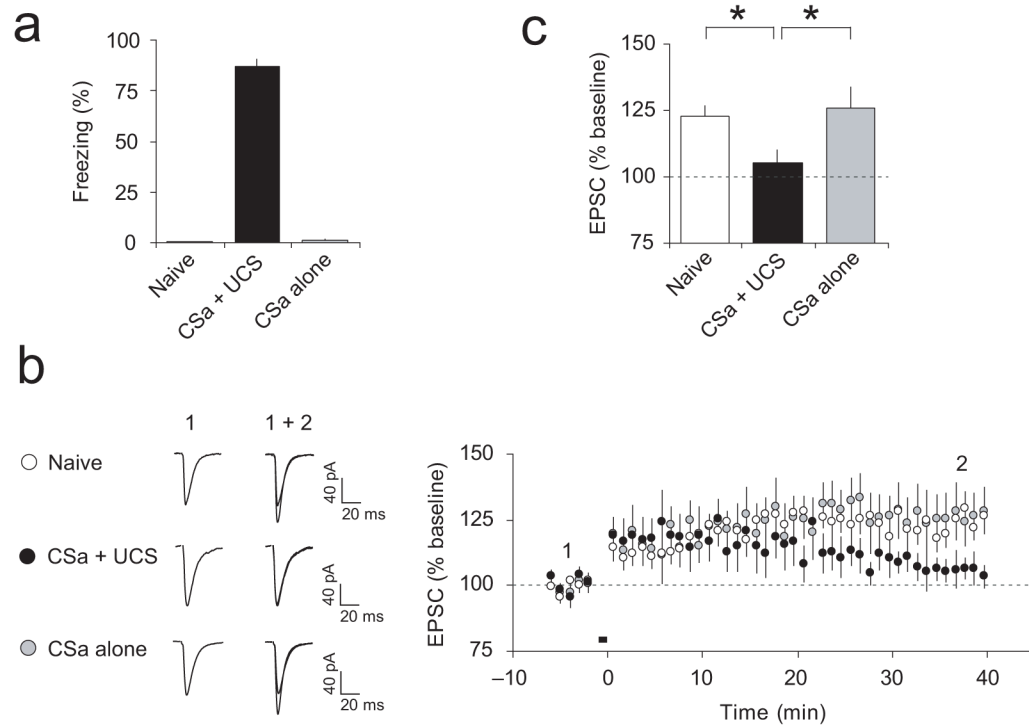
Author Manuscript

Author Manuscript

Author Manuscript



**Figure 7.** Fractional contribution of the AMPAR-, KAR-, and NMDAR-mediated synaptic components to the compound EPSP during the TSSt-CSt paired stimulation. **(a)** Examples of the EPSPs recorded in a LAN neuron in current-clamp mode evoked by paired stimulation of thalamic and cortical inputs with a 15 ms interval under control conditions (1) and in the presence of SYM 2206 (2), NBQX (3), and NBQX + D-AP5 (4). Responses were evoked once every 20 s. Note significant spatiotemporal summation of EPSPs during the TSSt-CSt paired stimulation. **(b)** Time course of the EPSP depression during application of SYM 2206, NBQX, and NBQX + D-AP5 (indicated by bars above the graph). Peak amplitude of EPSPs was normalized to the baseline EPSP amplitude ( $n = 6$ ). **(c)** Examples of isolated (subtracted) AMPAR-, KAR-, and NMDAR-mediated EPSPs from an experiment shown in **(a)**:  $EPSP_{AMPAR} = EPSP_{control} - EPSP_{SYM2206}$ ;  $EPSP_{KAR} = EPSP_{SYM2206} - EPSP_{NBQX}$ ;  $EPSP_{NMDAR} = EPSP_{NBQX} - EPSP_{NBQX+D-AP5}$ . **(d)** Fractional contribution of the AMPAR-, KAR-, and NMDAR-EPSPs in the compound EPSP (based on the peak amplitude measurements) during paired TSSt-CSt stimulation ( $n = 6$ ). Error bars indicate s.e.m.

**Figure 8.**

ITDP in cortico-LAN pathway is occluded in slices from fear-conditioned rats. **(a)** Freezing responses following single-trial auditory fear conditioning (CSa + UCS group) and freezing in behaviorally naïve rats and rats which received the CSa only. **(b)** Left, Representative cortico-LAN EPSCs (averages of 10 responses) recorded before (1) and after (2) the delivery of the TSt-CSt protocol ( $t = -15$  ms) in slices from all experimental groups (naïve, CSa + UCS, and CSa alone). Right, ITDP at the cortico-LAN synapses was occluded in slices from fear-conditioned rats ( $n = 12$  neurons from 8 rats, paired  $t$  test,  $P = 0.18$  versus the baseline amplitude), while significant ITDP was observed in behaviorally naïve rats ( $n = 14$  neurons from 9 rats,  $P < 0.001$  versus baseline) or the “CSa alone” rats ( $n = 7$  neurons from 4 rats,  $P < 0.05$  versus baseline). **(c)** Summary of the EPSC amplitude changes in cortical input following the TSt-CSt paired stimulation (as in **b**) in slices from different experimental groups of rats. \*  $P < 0.05$ , CSa + UCS group versus naïve or CSa alone group, one-way ANOVA with *post hoc* Bonferroni simultaneous tests. Error bars are s.e.m.